Determination of accurate, mean bond lengths from radial distribution functions

Sergey V. Sukhomlinov* and Martin H. Müser
Dept. of Materials Science and Engineering, Saarland University, 66111 Saarbrücken, Germany

The mean bond length d between a central atom and its nearest neighbors can be estimated from the position of the first peak in the radial distribution function $g(r)$. However, as we demonstrate here, this estimate does not allow one to deduce temperature-induced changes in d. Instead, skewness has to be included into the analysis, which can be achieved, for example, via the skew normal distribution (SND). Fits to the first peak using the SND give bond length in good agreement with direct measurements of nearest-neighbor distribution functions in crystals as well as with a Voronoi-tessellation based detection of nearest-neighbors in liquids. While the location of the first peak in $g(r)$ may shift to smaller values with increasing temperature for three studied liquids — argon, copper, and the bulk-metallic-glass (BMG) forming alloy $Zr_{60}Cu_{30}Al_{10}$ — we find our improved estimates of d to systematically increase with temperature in all cases. Recent conclusions on temperature-induced bond contractions in simple metallic or BMG-forming liquids may therefore have arisen from the neglect of skewness effects.

PACS numbers: 34.20.Cf, 02.70.Ns, 05.20.Jj, 65.40.-b

I. INTRODUCTION

Radial distribution functions (RDFs or $g(r)$) are routinely acquired in simulations and can also be deduced indirectly from X-ray spectra. An RDF states the probability density, divided by the mean number density, to find an atom at a randomly chosen point at distance r from a central atom. It provides incomplete, yet, useful information about the local order in liquids and solids alike. One piece of information sometimes obtained from the RDF is the mean distance or bond length d between two adjacent atoms.

In a recent paper [1], Lou *et. al.* found temperature-induced bond contractions in metallic melts, which they deduced from the observation that the maxima of partial RDFs moved to smaller radii upon heating. The authors correlated their observation with a reduction of the coordination number Z with increasing temperature T, which might indeed be meaningful: bonds generally shorten (roughly logarithmically) with increase of bond order [2], which is inversely proportional to Z in (simple) metals. Thus, if structural motifs with low coordination but large entropy become increasingly likely at high T, individual bonds between atoms could shorten on average. Similar observations were made for simple metallic liquids and various BMG forming melts [3, 4] as well as for ionic condensed-matter systems, such as UO_2 [5].

Previous studies of temperature-dependent bond lengths in small molecules revealed that the locations of the maxima in RDFs can indicate a thermal bond contraction while taking averages over the full probability distributions reveal bond stretching [6, 7]. In a similar spirit, Ding *et al.* [8] proposed that the perceived bond contraction in BMG-forming melts is due to the increase of peak asymmetry with temperature.

Two main difficulties arise with the interpretation of nearest-neighbor peaks in $g(r)$ of condensed-matter systems, except for crystals at low temperature: contributions from nearest neighbors and more distant neighbors to $g(r)$ overlap and individual peaks tend to deviate in a non-substantial way from Gaussians at elevated temperatures. An additional complication for fluids is that an unambiguous definition of a coordination number is not possible. It can yet be useful to rationalize the behavior of fluids in terms of local coordination. For example, the increasing viscosity of silica melts upon cooling can be linked to a decreasing number of coordination defects of silicon atoms [9].

This paper is concerned with the questions of how accurate conventional estimates of the average bond length are and how they can be improved. Towards this end we investigate various fits to $g(r)$ as well as to functions that can be deduced from $g(r)$ such as the function $\Pr(r)$ stating the probability density of finding another atom at any point with distance r from a central atom. Most importantly, we study how including skewness into the fitting of $\Pr(r)$ can benefit a meaningful determination of mean bond lengths and coordination numbers. For crystals, we can then compare directly the results of our fits to a reduced distribution function that only takes into account the distance between a central atom and its (topological) neighbors, which one can identify unambiguously as long as the window of observation is short compared to the time for two atoms to swap their lattice sites. For liquids, we use Voronoi tessellations in order to discriminate between nearest and next-nearest neighbors.

The remainder of this work is organized as follows: in section II we present background on various correlation functions and the skewed normal distribution function as well as details on our analysis and simulation methods. Section III contains results on three investigated model systems. Conclusions are drawn in the final section IV.

* s.sukhomlinov@fz-juelich.de

II. METHODS

A. Radial probability density

In this paper, we do not only consider the usual radial distribution function $g(r)$ but also the radial probability density (RPD) $\Pr(r)$ introduced above. The mathematical definition of the RPD for a mono-atomic system can be written as the following (thermal) expectation value

$$\Pr(r) \equiv \left\langle \sum_{n \neq m} \delta\left(r - r_{mn}\right), \right\rangle \tag{1}$$

where r_{mn} is the instantaneous distance between atoms m and n. In a three-dimensional system, $\Pr(r)$ fluctuates around but on average approaches $4\pi r^2 \rho_0$ at large r, where ρ_0 denotes the mean number density. The usual RDF, or, $g(r)$, relates to $\Pr(r)$ via

$$g(r) = \frac{\Pr(r)}{4\pi r^2 \rho_0}. \tag{2}$$

The reason why we focus on $\Pr(r)$ rather than on $g(r)$ is that it is the true probability density from which various quantities of interest can be directly deduced. For example, the integral over $\Pr(r)$,

$$Z(R) = \int_0^R dr \Pr(r), \tag{3}$$

states the (average) number of atoms lying within a sphere of radius R having a given atom in its center. $Z(R)$ can be loosely interpreted as a distance-dependent coordination number. Likewise, if one restricts the sum over n on the r.h.s. of equation (1) to (topological) nearest neighbors, the mean bond length can be directly deduced from the first moment of the resulting $\Pr_{\rm nn}(r)$ via

$$d = \frac{1}{Z} \int_0^\infty dr\, r \Pr_{\rm nn}(r). \tag{4}$$

Thus, when fitting to the RPD rather than to $g(r)$, analytical results on the first or higher moments of the assumed distribution function can be evaluated analytically without further numerical integration.

B. Properties of the skew normal distribution and fitting of individual peaks

Individual peaks of radial distribution functions are sometimes fitted to Gaussians. The deduced information can be quite inaccurate, whenever peaks reveal a non-negligible skewness, in particular when considering actual probability densities $\Pr(r)$ rather than $g(r)$. The skew normal distribution (SND) [10, 11] is arguably the simplest distribution for which the first three moments of a distribution can be fit simultaneously, while reproducing the Gaussian distribution in the limit of zero skewness. The SND is defined as

$$f_{\rm SND}^{(\mu,\sigma,\xi)}(x) = \frac{e^{-(x-\mu)^2/2\sigma^2}}{\sqrt{2\pi\sigma^2}} \left[1 + \mathrm{erf}\left(\xi \frac{x-\mu}{\sigma}\right)\right], \tag{5}$$

where μ, σ, and ξ are the three coefficients determining the first two moments of the random variable x, that is, $\bar{x}$ and $\langle (x-\bar{x})^2 \rangle$, as well as the skewness γ of its distribution. Specifically

$$\bar{x} = \mu + \sqrt{\frac{2}{\pi}} \sigma \tilde{\xi} \tag{6}$$

$$\left\langle (x-\bar{x})^2 \right\rangle = \sigma^2 \left(1 - \frac{2}{\pi}\tilde{\xi}^2\right) \tag{7}$$

$$\gamma = \frac{4-\pi}{2} \frac{\tilde{\xi}^3}{\left(\pi/2 - \tilde{\xi}^2\right)^{3/2}} \tag{8}$$

with $\tilde{\xi} = \xi/\sqrt{1+\xi^2}$.

In (defect-free) crystals, atoms fluctuate around well-defined positions so that each neighbor shell contributes one SND. The total probability density then becomes

$$\Pr(r) \approx \sum_{s=1} Z_{\rm s} f_{\rm SND}^{(\mu_s,\sigma_s\xi_s)}(r), \tag{9}$$

where $Z_{\rm s}$ is the number of atoms in shell s, starting the enumeration of s at $s = 1$ for the nearest-neighbor shell. Each shell can then be assigned its individual set of parameters μ_s, σ_s, and ξ_s.

C. Voronoi tessellation analysis

Voronoi tessellations [12] are frequently used to characterize local order in disordered condensed matter such as liquids and glasses [13]. They allow one to classify the surrounding of atoms to resemble that of a face-centered-cubic (fcc) crystal if the Voronoi polyhedra with these atoms in their centers correspond to rhombic dodecahedrons. Similarly, if the local order is comparable to that of a body-centered-cubic (bcc) crystal, one would expect polyhedra resembling truncated octahedra.

The rhombic dodecahedrons of ideal fcc lattice sites have twelve faces perpendicular to the nearest-neighbor bonds of area $2^{-7/6} \times \rho_0^{-2/3}$. Voronoi polyhedra of an ideal fcc lattice is not topologically stable with respect to infinitesimal perturbations of the lattice points positions: when thermal fluctuations perturb the ideal fcc structure, the polyhedra deforms and may have up to six more faces related to the next-nearest neighbors, and also twelve polyhedra faces fluctuate in size. For large fluctuations, it may well happen that a face associated with a next-nearest neighbor is larger than that of a nearest neighbor. This, however, we find to happen much less frequently than next-nearest-neighbor bonds to become shorter than those associated with (topological) nearest

neighbors. One may therefore conclude that a Voronoi-based identification of nearest neighbors can be made more reliable than those based on distances.

The two elemental liquids of interest studied in this work, namely argon and copper, both have fcc crystalline reference phases. We want our tessellation scheme to produce accurate estimation for the correct coordination number when applying it to an fcc crystal close to melting. As long as fluctuations in this crystal are small, this can be achieved by excluding all atoms from the nearest-neighbor list whose associated face areas are less than an appropriate fraction f of the mean — or an approximation of the mean — of the $Z = 12$ face areas $\bar{a}$ belonging to nearest neighbors.

To fully define how nearest neighbors shall be identified, we need to come up with a recipe for how to construct $\bar{a}$ and we also need to state a meaningful value of f. There is much ambiguity and perhaps no ideal solution. The reason is that the situation is even not simple for crystals: close to melting, fluctuations of the face areas might be so large that the face of a next-nearest neighbor is larger than that of a nearest neighbor. In that case, no criterion solely based on the (instantaneous) Voronoi-face area will be in a position to categorize the neighbors correctly. We choose $\bar{a}$ as the average value of the 6'th and 7'th largest face, and pick f to be the ratio of the areas associated with a small and a large face in bcc ($f = 2/\sqrt{27}$).

We note that results actually do not depend very sensitively on the details of how $\bar{a}$ and f are acquired as long as they are "reasonable" for the given system. For the analysis of amorphous carbon with typical coordination numbers of three or four, our choices would certainly not work. Yet, we observed that designing a recipe leading to relatively small values of $f\bar{a}$ lead to larger estimated coordination numbers and also larger bond lengths than for larger values of $f\bar{a}$, which is easily explained: reduction of $f\bar{a}$ leads to the inclusion of more distant atoms, which extends the long distance tail of the distribution and thus increases its skewness. However, the way in which Z and d changed with temperature turns out to be very similar for all tested scenarios – mainly argon and copper.

D. Investigated systems and potentials

We investigate two simple fluids and one three-component melt, each of which with an appropriate potential. The first model is a pair potential, namely, a simple 12-6 Lennard-Jones (LJ) potential representative of argon. Second, we employ a bond-order potential originally proposed by Gupta [14], which can be seen as a generic many-body potential for simple metals. It produces the (dimensionless) properties — such as the ratio of shear and bulk modulus or the ratio of vacancy and cohesive energy — of quite a few metals [15]. It is arguably the simplest potential with which one can model the logarithmic increase of bond length with coordination number; this is in contrast to most simple pair potentials like LJ, which tend to decrease d with Z due to next-nearest neighbor interactions. Lastly, we study the BMG-forming alloy $Zr_{0.6}Cu_{0.3}Al_{0.1}$ with an embedded-atom potential that was specifically designed for Zr-Cu-Al alloys [16].

All simulations are run in the NpT ensemble, the two mono-component systems with a house-written code and the Zr-Cu-Al using LAMMPS [17]. We study the crystalline and fluid phases of argon and copper in temperature regimes, in which the respective phase can be kept (meta-) stable for a few nanoseconds. Since periodic boundary conditions impede nucleation of bubbles, or crystallization from the surfaces, liquids can be investigated much beyond their thermodynamic stability, i.e., fluids can be strongly overheated or undercooled. Likewise, solid phases can be overheated quite substantially, amongst other reasons, because vacancies cannot be generated without interstitials, thereby suppressing the generation of defects necessary for melting. Crystals are only simulated with ideal particle numbers, e.g., by setting up $6 \times 6 \times 6$ elementary cells each containing 4 atoms. As a consequence, no (stoichiometric) vacancies or interstitial defects exist in our simulations cells. For the BMG-forming ternaries, we consider predominantly equilibrium melts.

III. RESULTS

A. Solid argon

We first demonstrate in figure 1 that the RPD of a defect-free solid can be very well represented by a sum over skewed-normal distributions according to equation (9), even at very high temperatures. In fact, the shown data relates to an argon crystal, which is superheated roughly 2 K above the solid-liquid transition of 83 K. We note that the skewness effects quickly become less relevant as the (crystallographic) distance between the central atom and a neighbor increases. However, there is also a directional dependence. Specifically, the skewness parameter for the explicitly shown shells are $\xi_1 = 3.44$, $\xi_2 = 0.029$, $\xi_3 = 1.42$, and $\xi_4 = 0.01$.

We next address the question of how well different strategies to deduce bond lengths relate to an "exact measurement". The latter is conducted in the crystalline phase by taking histograms only over those pairs of atoms that are topological neighbors. This is done as follows: when atoms are placed onto their crystallographic positions in the beginning of the simulation, each atom memorizes its neighbors. Averages and histograms are then acquired over a time that is sufficiently long to produce very smooth curves but shorter than diffusive time scales allowing two atoms to swap their place. Although this analysis cannot be applied to fluids, it reveals unavoidable errors in the proposed skewness fits, e.g., those that occur when only fitting to a part of the nearest-neighbor

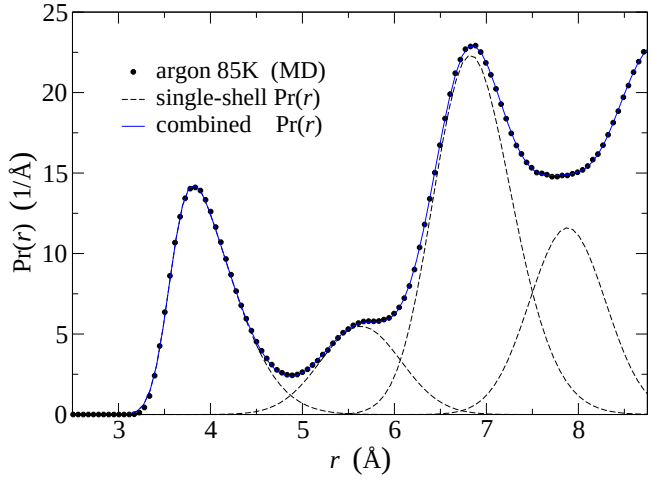

FIG. 1. Decomposition of the radial probability density $\Pr(R)$ of superheated crystalline argon at 85 K into contributions belonging to different neighbor shells according to equation (9).

peak.

The following procedures are conducted to deduce a mean bond length d: It is associated with or obtained from (i) the location at which $g(r)$ is maximum, (ii) the most likely bond length, i.e., the position where $\Pr(r)$ is maximum, (iii) the fit of a Gaussian to $\Pr(r)$, (iv) a Voronoi-tessellation based analysis, (v) the distance between two adjacent crystallographic positions, i.e., $d \approx (4\langle\rho_0^{-1}\rangle)^{1/3}/\sqrt{2}$ for fcc, (vi) the fit of $\Pr(r)$ to a skew normal distribution, and (vii) the direct averaging as described in the precedent paragraph. Results are presented in figure 2.

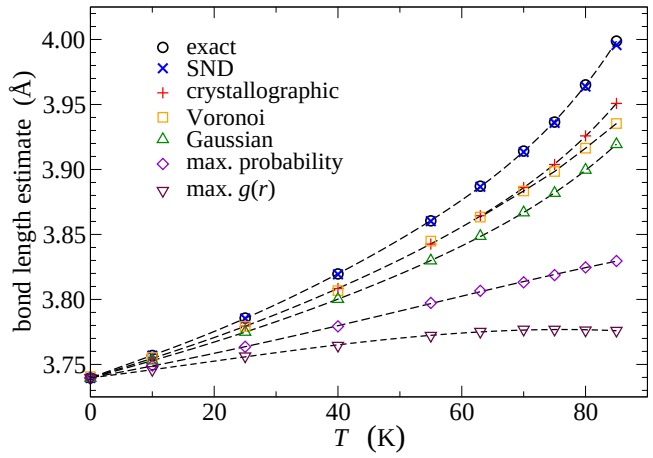

FIG. 2. Bond length estimates for crystalline argon at various temperatures based on direct averaging (black circles), SND fit to the Pr(r) (blue crosses), distance between two crystallographic positions (red pluses), Voronoi-tessellation analysis (orange squares), fit of a Gaussian to Pr(r) (green triangles up), position of the first maximumin Pr(r) (purple diamonds) and position of the first maximum position in $g(r)$ (maroon triangles down). Dashed lines are drawn to guide the eye.

Figure 2 shows that the SND-based fit to the nearest-neighbor distribution function reproduces very accurately the direct bond-length measurement. The next two best approximations are obtained from the crystallographic positions and Voronoi tessellations followed by a Gaussian fit to the full nearest-neighbor $\Pr(r)$. Thermal expansion of the mean bond length is reproduced semi-quantitatively by either of the two methods. However, deducing thermal expansion from maxima of $\Pr(r)$, or even worse, from $g(r)$, produces errors close to - and sometimes exceeding - 100%.

In general, one might not be in a position to generate histograms resolving what part of $g(r)$ comes from atoms in which shell. One might not even know the exact occupation number of the nearest or next-nearest neighbor shell. In this situation, the coordination number of a shell becomes an adjustable parameters in addition to the parameters μ_s, σ_s, and ξ_s. To test how well-informed initial guesses for the first shell produces reasonable numbers on local bonding, we pursue a strategy that is similar to the one that we later take for disordered systems. The main idea is to first obtain a rough guess for the nearest-neighbor peak and then to model the "medium-range" range density oscillation, which finally allows for a reoptimization of the first peak. Towards this end, we focus on $T = 80$ K, which is just a little below the experimental melting temperature of 83.8 K.

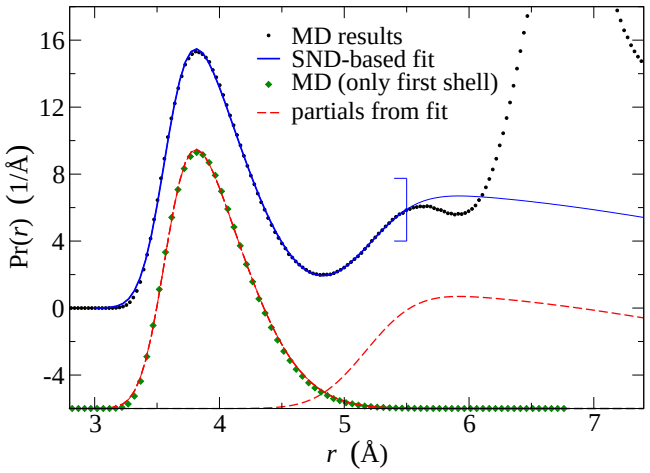

FIG. 3. Comparison of fits (blue, solid lines) and directly measured $\Pr(r)$ (small, black circles) for argon crystal at $T = 80$ K. The fits only consider data for $r \leq 5.5$ Å. Partials are also shown, first and second SND-peaks (red, broken line) and first-neighbor peak (small, green diamonds). The partials are shifted below to improve the clarity of the figure.

In the case of crystalline argon, with fcc as reference phase, we proceed as follows: We first restrict the fitting range to $r < 4.2$ Å and pretend to not know the precise coordination number. The first iteration leads to estimates of $Z_1 = 12.42$ and a mean bond length of $d = 3.7396$ Å. We next increase the domain of integration to the second maximum of $g(r)$, i.e., to $r \leq 5.5$ Å,

and adjust Z_2, μ_2, σ_2, and ξ_2. Although, we start with a well-informed guesses, ($Z_2 = 6$, $\mu_2 = \sqrt{2}\mu_1$, $\sigma_2 = \sigma_1$, and $\xi_2 = \xi_1/2$) a very broad, rather skewed distribution is obtained. The resulting distribution is presented in figure. 3. We finally readjust the parameters characterizing both shells and now find $Z_1 = 12.15$, $d = 3.9637$ Å, which compares well to the exact results of $Z_1 = 12$, $d = 3.9651$ Å. In fact, although we did not include any information on what part of Pr(r) came from which shell, the contribution of the nearest-neighbor shell to the total Pr(r) is reproduced almost exactly. By including information on the fluctuations of Pr(r) beyond those parts that can be clearly identified to belong to the first peak, initial errors on predicted coordination numbers (3.5%) and bond lengths (5.7%) could thus be reduced to 1.2% and 0.03%, respectively.

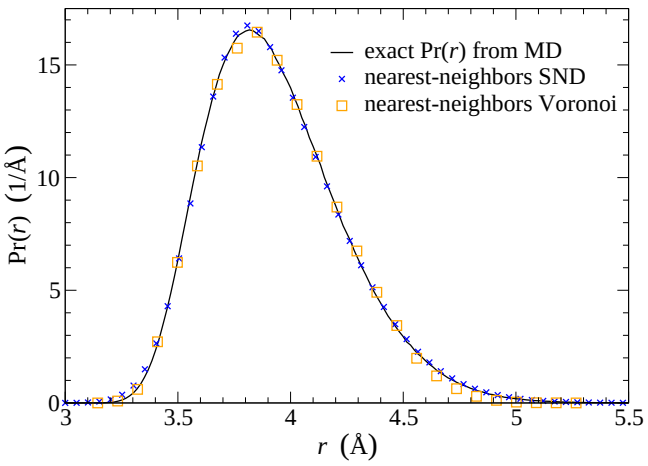

FIG. 4. Distribution of nearest-neighbor peak of solid argon at 75 K as deduced exactly from molecular dynamics (black lines) as well as from a screw-normal distribution fit to the first peak (SND) and from a Voronoi analysis (orange squares).

We applied the same procedure to the crystalline argon at $T = 75$ K. The resulting first peak of the Pr(r) for was then compared to the exact distribution obtained from molecular dynamics as well as with the Voronoi-tessellations analysis. From figure. 4 one can conclude that the three methods agree well. The skewness fit slightly overestimates the likelihood of small inter-atomic distances while the Voronoi tessellation underestimates the true Pr(r) at large distances.

B. Liquid Argon

We repeat our analysis of the RPD of crystalline argon for the liquid phase. This time, however, one cannot identify topological nearest neighbors so that the assessment of bond length is not uniquely defined. One may nevertheless appreciate in figure 5 that an SND fit to the first peak and the Voronoi-tessellation based analysis give rather similar estimates for what part of Pr(r) should be related to nearest neighbors.

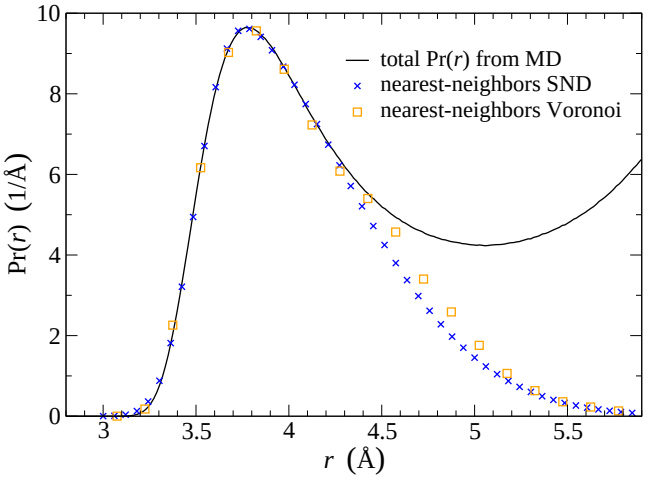

FIG. 5. Full distribution function Pr(r) of liquid argon at $T = 85$ K as measured from MD simulations (black line) and partial distribution functions as deduced from a SND fit to the nearest-neighbor peak (blue crosses) and from a Voronoi tessellation (orange squares).

Analysis, such as those presented in figure 5 were repeated in a broad temperature regime. The respective SND-based fits to the first peak in Pr(r) are shown in figure 6 from a strongly undercooled liquid at $T = 55$ K to an overheated liquid at $T = 110$ K. In this range, the SND gives a rather accurate representation of the RPD.

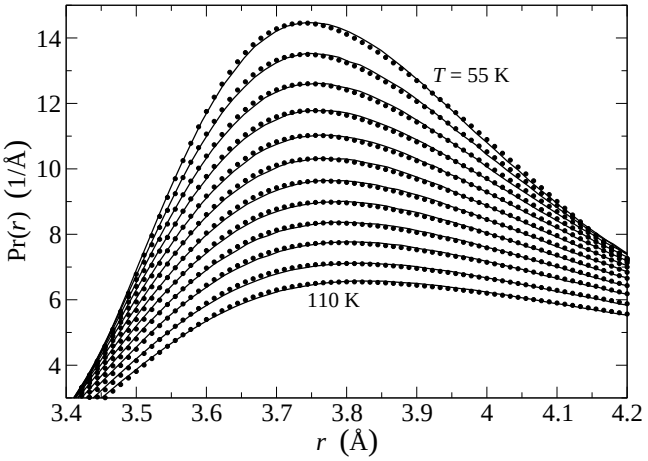

FIG. 6. SND fits (circles) to the first peak of Pr(r) in liquid (supercooled, stable, and superheated) argon from $T = 55$ K to $T = 110$ K – in steps of 5 K. The SND was adjusted to the MD data (full lines) in the range $r < 4.2$ Å. The fits also target data to smaller radii than those shown.

Different estimates for the bond length in liquid argon are presented in figure 7. As is the case for solid argon, the location of the first maximum of $g(r)$ gives reasonable zero-order guesses for the bond length, but it does not

reflect the thermal expansion correctly. The maximum-$g(r)$ analysis gives relatively temperature-independent values of d slightly exceeding 3.7 Å. Conversely, both Voronoi-tessellations and the SND-based analysis of the first RPD peak suggest the expected thermal bond expansion. Each time, the data is similar to that obtained for the crystalline reference system.

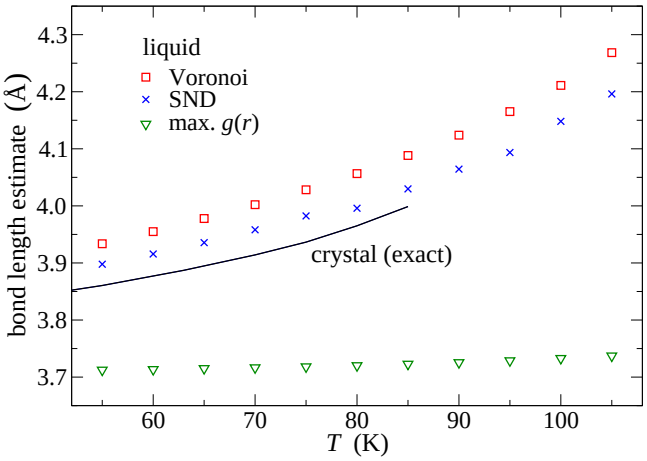

FIG. 7. Estimates for the bond length d in liquid (supercooled, stable, and superheated) argon using a Voronoi tessellation analysis (red squares), SND fit to the first peak in Pr(r) (blue crosses), and the location of the maximum in the radial distribution function $g(r)$ (green triangles).

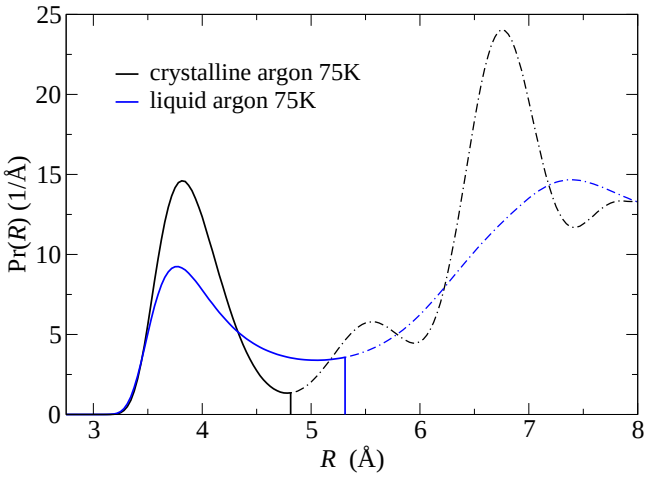

FIG. 8. Probability density distribution function Pr(r) of crystalline (black line) and liquid (blue line) argon. Vertical lines correspond to the position of the first minimum in the radial distribution function $g(r)$.

Tröger *et. al.* [18] introduced a method for estimating the average bond length from RDFs, which we have not yet discussed. d is set equal to the first moment of the probability density distribution function Pr(r) on the interval from zero to the first minimum of the radial distribution function $g(r)$. An example of the procedure is illustrated in figure 8. Positions of the first minimum of $g(r)$ are marked by vertical lines. One can clearly see that this moment-based method can give quite reasonable numbers for crystals, since the overlap of the first and the second peak is relatively small. However, the position of the first minimum of $g(r)$ in the liquid phase is located almost (as it is also the case for copper and probably any other element condensing in fcc) at a position that is close to the crystalline second-neighbor peak. This leads to a significant overestimation of the average bond length in the liquid. To illustrate this point better, we provide quantitative results: the current method predicts an increase of d by 0.25 Åfrom the crystalline stable phase to the liquid metastable phase at 75 K. Such a large elongation of the bond length in argon is not physical and in fact exceeds the bond length increase from an SND fit or the Voronoi analysis by a factor of six. Moreover, in some cases this method will give the wrong sign for the skewness of the distribution. We therefore do not see the moment-based approach as useful for the analysis of liquids.

C. Solid and liquid copper

Results on the bond lengths for solid copper reveal much similarity with those obtained for argon, at least when using an appropriate reduced unit system. This could certainly be expected since both elements condense in the fcc structure. Quantitative differences occur nevertheless. They are surprisingly minor given that the LJ potential for argon is a two-body potential while that used for copper is a many-body potential. We abstain from repeating the detailed analysis of the last two sections and instead focus on selected results as well as their analysis.

Figure 9 shows that copper bond lengths appear to contract thermally when they are evaluated by locating the maximum of $g(r)$. The effect is particularly strong for the liquid. However, the more refined estimates based on Voronoi tessellations or an SND analysis of the RPD show qualitatively the same behavior as that found in solids, for which bond lengths can be computed without ambiguity. In fact, we expect that any elemental metal or even semi-metal would behave qualitatively similar to copper in that regard.

We next analyze to what extent the overall thermal expansion correlates with the bond length increase. Towards this end, we show a reduced density $\rho_{\rm r}(T) \equiv \rho(T)d^3(T)/\sqrt{2}$ in Figure 10 as a function of temperature. It is designed such that $\rho_{\rm r}(T)$ would be constant if the sole effect of temperature would be to increase the bond lengths without changing any (distribution of) bond angles, vacancy occupancies, local structural motifs, etc. $\rho_{\rm r}$ is normalized such that it is equal to one for an ideal fcc lattice, i.e., when the bond length estimate $d(T)$ is deduced from the crystallographic positions $\rho_{\rm r} \equiv 1$.

When using the mean *instantaneous* bond length of the

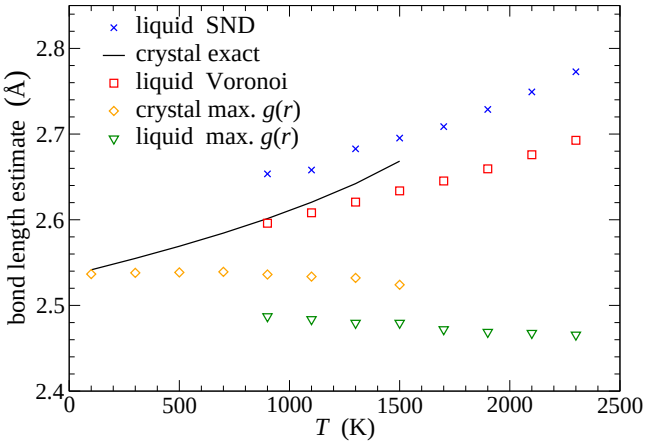

FIG. 9. Estimates for the bond length d in copper using SND fit to the first peak in Pr(r) for liquid (blue crosses), Voronoi tessellation analysis for liquid (red squares), the location of the maximum in the radial distribution function $g(r)$ for crystal (orange diamonds), and the location of the maximum in the radial distribution function $g(r)$ for liquid (green triangles).

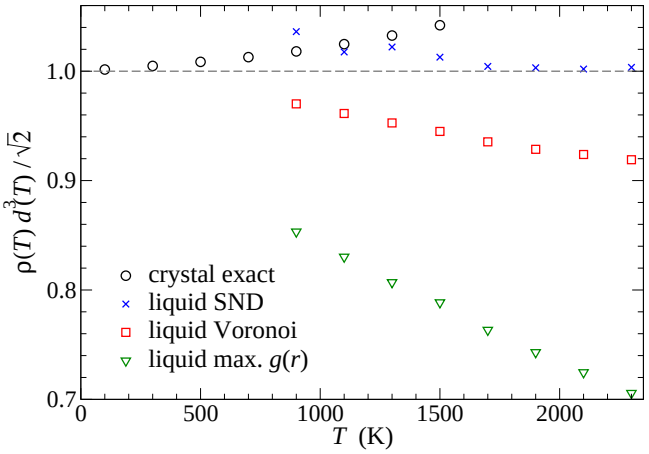

FIG. 10. Temperature dependence of the density $\rho(T)$ expressed in units of $\sqrt{2}/d^3(T)$. When deducing $d(T)$ from the ideal crystallographic position, this reduced density would be strictly one – as indicated by the grey, dashed line. Other symbols refer to mean, instantaneous bond lengths in the crystal (black circles), SND fits to the first peak in Pr(r) (blue crosses), Voronoi tessellation analysis (red squares), and the location of the maximum in the radial distribution function $g(r)$ (green triangles).

crystal or the SND-based estimate for d in the liquid, ρ_r does not show much of a temperature dependence and turns out close to the value of one, which one would expect if local packing were similar to that in fcc. However, when using the maximum of $g(r)$ to estimate d, ρ_r falls much below unity at elevated temperature. When postulating an fcc-type local order in the liquid, one would have to conclude that liquid expansion is driven primarily by the formation of "voids", as proposed by Bar'yakhtar et. al. [19]. However, this conclusion is not supported when estimating d in a more sophisticated fashion such as through an SND or Voronoi analysis.

The reduced density ρ_r shows a slight decrease in the SND and Voronoi analysis with increasing temperature, indicative of a less tight packing at high T than at low T. Though the deduced trend is much smaller than when using the maximum of $g(r)$ for this analysis. In fact, coordination numbers deduced from either SND or Voronoi in the liquid phase do show a slight decrease with T – to values of roughly 11 near the melting temperature – while the maximum $g(r)$ analysis might have tempted one to believe coordination numbers would be smaller by as much as 30%. Values of the reduced packing density greater than one might be seen to contradict the fact that packings (of hard spheres) cannot be denser than that of fcc. However, the SND-based predictions of a reduced packing density exceeding one are allowed since our atoms are not hard spheres and vibrate thermally. See also figure 2, where the crystallographic bond lengths are less than the mean instantaneous bond lengths.

D. BMG-forming Zr-Cu-Al melt

So far, we have only investigated elemental systems. Compounds, such as BMG forming alloys, might be more complex and reveal thermally induced bond contraction, as proposed recently [1]. To investigate this issue, we consider an equilibrium melt of the generic BMG former $Zr_{0.6}Cu_{0.3}Al_{0.1}$.

One difficulty when studying alloys is that the experimentally deduced radial distribution function can be (roughly) seen as a weighted superposition of individual partial distribution functions. Only scientists who run simulations (and experimentalists who can afford to repeat neutron scattering experiments with different isotopes) are in a position to measure each partial distribution function individually. In order to ascertain what "effective" bond length one might perceive based on the superposition of individual $g(r)$'s, we define and study a distribution function, for which Zr is the central atom, but all neighbors are assigned the same weight, irrespective of its chemical nature. Fits to such compound Pr(r) with skewed Gaussians may not always be justified for alloys (e.g., there is the possibility for the splitting of the first peak into a double or triple peak), but for our system, it was sufficiently good – and yielded similar results as for the analysis of distribution functions that were chemically fully resolved into, e.g, Zr-Zr or Zr-Cu contributions.

As was the case in the elemental systems, we find that sophisticated methods to estimate bond length suggest that $d(T)$ is a strictly increasing function with T, while analysis of the maximum of $g(r)$ would have again indicated a thermally induced bond contraction, see in figure 11.

Note that we slightly modified the Voronoi nearest-

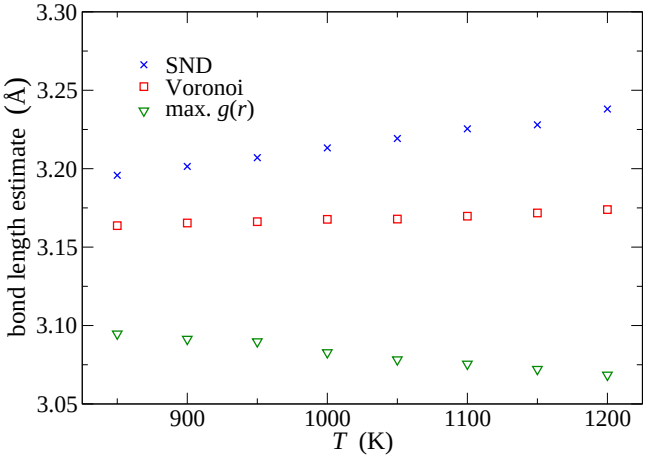

FIG. 11. Estimates for the bond length in BMG-forming melt between Zr atom and its neighbors using SND fit to the first peak in Pr(r) (blue crosses), a Voronoi tessellation analysis (red squares), and the location of the maximum in the radial distribution function $g(r)$.

neighbor determination for Zr atoms in the alloy, because the average Zr-Zr, Zr-Cu, and Zr-Al distances are all different, which leads to a strong deformation of the constructed nearest-neighbor polyhedra. We therefore reduced the value of f to $f = 0.2$ by almost a factor of two. Individual snapshots gave a more meaningful classification into nearest and next-nearest neighbors, and, at the same time, the deduced nearest-neighbor distribution function resembled somewhat better that deduced of the SND fits, as shown in figure 12.

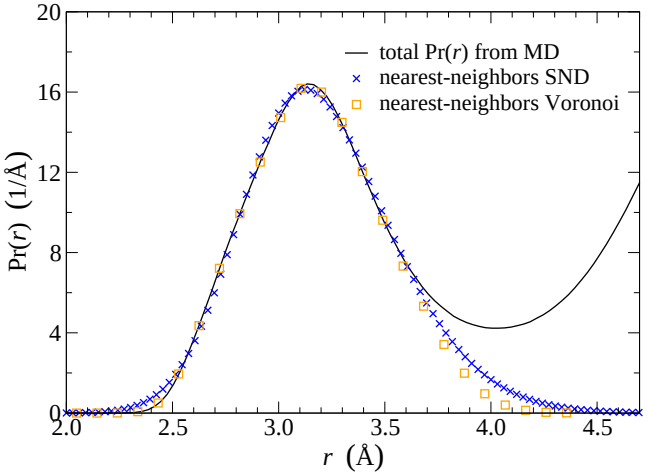

FIG. 12. Distribution function Pr(r) of BMG-forming melt with Zr atoms being treated as central at $T = 950$ K as measures from MD simulations (black line) and partial distribution functions as deduced from the SND fit to the nearest-neighbor peak (blue crosses) and from a Voronoi tessellation (orange squares).

In the case of a three-component system, the Voronoi construction is certainly more meaningful than the SND fit (which really should be a superposition of three skewed Gaussians). The SND nearest-neighbor partial nevertheless reflects the Voronoi partial relatively closely and might be the sole option of analysis when the only available information is the static structure factor from which some estimate for $g(r)$ or $\mathrm{Pr}(r)$ needs to be deduced.

IV. CONCLUSIONS

In this article, we critically investigated the validity of recent speculations that bonds in metallic melts [1, 20] and BMG-forming melt [3, 4, 21] contract upon a temperature increase. The conclusions had been drawn on the analysis of how the first maximum position of $g(r)$ shifts under a temperature change. While our simulations reproduced the apparent bond contraction, i.e., a shift of the location of the first peak in $g(r)$ to smaller r at higher temperature, more refined analysis revealed that "true" bond lengths increased with temperature in all investigated systems. These results are in agreement with conclusions drawn by Ding *et al.* [8], who convincingly demonstrated that skewness, or, more generally, asymmetry can lead to a larger first shell than estimates based on the first maximum of $g(r)$ would convey, see their figure 5.

To conduct our analysis, we proposed – and tested – that mean bond lengths can be deduced by fitting individual peaks of the radial probability function $\mathrm{Pr}(r)$ with the skewed normal distribution, which contains the Gaussian distribution as a limiting case. Results based on such fits revealed much similarity with direct bond measurements in crystals but also with bond-length measurements that were deduced from Voronoi tessellations. Using the SND or Voronoi-tessellations based analysis, we found that bond lengths in all studied systems, namely argon, copper, and the BMG-forming $Zr_{0.6}Cu_{0.3}Al_{0.1}$ alloy always expand – in liquid and solid phases alike – when raising the temperature. While we could describe the first peak in $\mathrm{Pr}(r)$ in liquid argon and liquid copper relatively close to their boiling point at ambient pressures, we would be reluctant to apply our SND analysis to systems of even lower density, e.g., those in the vicinity of a critical point. The reason is that a meaningful validation against Voronoi tessellations is no longer possible when a system becomes so rare that internal gas bubbles occur with a non-negligble probability.

A quantitative difference between argon and the metallic systems is that the skewness effects are somewhat smaller in argon than in the metals. Specifically, they are not large enough to fully induce an apparent bond contraction in liquid argon but only a (strong) reduction of the perceived bond expansion. We rationalize this as follows: The interaction between two argon atoms – when modeled with LJ potentials – does not depend on the location of other atoms. This is different for metallic interactions: the bond between two metal atoms becomes weaker (stronger) when other metal atoms approach (be-

come more distant) from that original pair. As such the three or four closest atoms become tightly bonded to a central atom when other neighbors distance themselves very far through a large fluctuation. This can lead to a relatively pronounced peak at a short bonding distance and large skewness effects in the nearest-neighbor distribution function. The argument is not specific to the investigated elements but supposedly applies in similar form to other metals and potentially even to covalently bonded systems, such as liquid carbon.

We conclude that the proposed SND analysis of nearest neighbor distances is a useful tool to assess bond lengths from radial distribution functions, or, to be precise from the radial probability distribution. The SND analysis might be particularly helpful when the full microscopic information is not at hand but, for example, only the static structure factor, which does not put one into a position to conduct Voronoi tessellations.

ACKNOWLEDGMENTS

We thank Moritz Stolpe, Isabella Gallino and Ralf Busch for useful discussions and the German Research Science foundation (DFG) for financial support through Grant No. Mu 1694/6-1.

[1] H. Lou, X. Wang, Q. Cao, D. Zhang, J. Zhang, T. Hu, H. k. Mao, and J.-Z. Jiang, Proceedings of the National Academy of Sciences **110**, 10068 (2013).
[2] L. Pauling, J. Am. Chem. Soc. **69**, 542 (1947).
[3] A. K. Gangopadhyay, M. E. Blodgett, M. L. Johnson, J. McKnight, V. Wessels, A. J. Vogt, N. A. Mauro, J. C. Bendert, R. Soklaski, L. Yang, and K. F. Kelton, The Journal of Chemical Physics **140**, 044505 (2014).
[4] M. Blodgett and K. Kelton, Journal of Non-Crystalline Solids **412**, 66 (2015).
[5] L. B. Skinner, C. J. Benmore, J. K. R. Weber, M. A. Williamson, A. Tamalonis, A. Hebden, T. Wiencek, O. L. G. Alderman, M. Guthrie, L. Leibowitz, and J. B. Parise, Science **346**, 984 (2014).
[6] K. Kuchitsu and L. S. Bartell, The Journal of Chemical Physics **35**, 1945 (1961).
[7] L. S. Bartell, Journal of Molecular Structure **84**, 117 (1982).
[8] J. Ding, M. Xu, P. F. Guan, S. W. Deng, Y. Q. Cheng, and E. Ma, The Journal of Chemical Physics **140**, 064501 (2014).
[9] J. Horbach and W. Kob, Phys. Rev. B **60**, 3169 (1999).
[10] A. O'Hagan and T. Leonard, Biometrika **63**, 201 (1976).
[11] G. S. Mudholkar and A. D. Hutson, Journal of Statistical Planning and Inference **83**, 291 (2000).
[12] F. C. Frank and J. S. Kasper, Acta Crystallogr **11**, 184 (1958).
[13] H. W. Sheng, W. K. Luo, F. M. Alamgir, J. M. Bai, and E. Ma, Nature **439**, 419 (2006).
[14] R. P. Gupta, Phys. Rev. B **23**, 6265 (1981).
[15] S. V. Sukhomlinov and M. H. Müser, Journal of Physics: Condensed Matter **28**, 395701 (2016).
[16] Y. Q. Cheng, E. Ma, and H. W. Sheng, Phys. Rev. Lett. **102** (2009), 10.1103/physrevlett.102.245501.
[17] S. Plimpton, Journal of Computational Physics **117**, 1 (1995).
[18] L. Tröger, T. Yokoyama, D. Arvanitis, T. Lederer, M. Tischer, and K. Baberschke, Phys. Rev. B **49**, 888 (1994).
[19] V. G. Bar'yakhtar, L. E. Mikhailova, A. G. Ilinskii, A. V. Romanova, and T. M. Khristenko, Zh. Eksp. Teor. Fiz. **95**, 1404 (1989).
[20] D. V. Louzguine-Luzgin, K. Georgarakis, A. Tsarkov, A. Solonin, V. Honkimaki, L. Hennet, and A. R. Yavari, Journal of Molecular Liquids **209**, 233 (2015).
[21] J. Tan, G. Wang, Z. Y. Liu, J. Bednarčík, Y. L. Gao, Q. J. Zhai, N. Mattern, and J. Eckert, Sci. Rep. **4** (2014), 10.1038/srep03897.